EUROPEAN JOURNAL OF CANCER 48 (2012) 772–781

Available at www.sciencedirect.com

SciVerse ScienceDirect

journal homepage: www.ejconline.com

Aquaporin-4 expression in primary human central nervous system lymphomas correlates with tumour cell proliferation and phenotypic heterogeneity of the vessel wall

Beatrice Nico [a,*], *Tiziana Annese* [a], *Roberto Tamma* [a], *Vito Longo* [b], *Simona Ruggieri* [b], *Rebecca Senetta* [c], *Paola Cassoni* [c], *Giorgina Specchia* [d], *Angelo Vacca* [b], *Domenico Ribatti* [a,*]

[a] *Department Basic Medical Sciences, Section of Anatomy and Histology, University of Bari Medical School, Bari, Italy*
[b] *Department of Internal Medicine and Clinical Oncology, University of Bari Medical School, Bari, Italy*
[c] *Department of Biomedical Sciences and Human Oncology, University of Turin Medical School, Italy*
[d] *Hematology Section, Department of Pathology and Hematology, University of Bari Medical School, Bari, Italy*

ARTICLE INFO

Article history:
Available online 17 November 2011

Keywords:
AQP4
Angiogenesis
Cerebral lymphomas
Ki-67
Tumour microvasculature

ABSTRACT

No literature data are available concerning the expression of aquaporin-4 in primary central nervous system lymphomas and the relationship between aquaporin-4 expression and the morphological characteristics of blood vessels. Here, we have investigated this relationship in 24 human diffuse large B-cell primary central nervous system lymphomas by means of immunocytochemistry and confocal laser microscopy. Results have shown that: (i) a high aquaporin-4 expression correlated with a high Ki-67 index and aquaporin-4 marked tumour and endothelial cells in cytoplasm and plasma membranes, while aquaporin-4 expression was low in tumour areas with a low Ki-67 index where few tumour cells were positive to aquaporin-4, and endothelial cells showed aquaporin-4 expression on their abluminal side. (ii) Different type of cells participated in vessels formation: $CD20^+$ tumour cells and factor $VIII^+$ endothelial cells; $aquaporin\text{-}4^+$ tumour cells and $CD31^+$ endothelial cells; $CD20^+$ and $aquaporin\text{-}4^+$ tumour cells; glial fibrillary acidid $protein^+$ endothelial cells surrounded by glial fibrillary $acidic\ protein^+$ tumour cells. Overall, these data suggest the importance of aquaporin-4 in primary central nervous system lymphomas due to its involvement in cerebral oedema formation and resolution and tumour cell migratory activity, and have documented that tumour microvasculature in lymphomas is extremely heterogeneous, confirming the importance of neoangiogenesis in the pathogenesis of lymphomas.

1. Introduction

Lymphomas constitute a large group of more than 40 heterogeneous lymphoproliferative disorders. Primary central nervous system lymphoma (PCNSL) is an extranodal non-Hodgkin's lymphoma (NHL) arising in the central nervous system (CNS) in the absence of lymphoma outside the CNS at the time of diagnosis. The majority of PCNSL would be classified as diffuse large B-cell lymphomas.[1]

The importance of angiogenesis in human lymphomas relates to the association of disease progression with increased angiogenic activity.[2] Tumour vascularisation is higher in lymphoma tissue than in reactive lymph nodes and increases in step with more aggressive subtypes and advanced stage

* *Corresponding authors:* Address: Department of Basic Medical Sciences, Section of Human Anatomy and Histology, University of Bari Medical School, Piazza G. Cesare, 11 Policlinico, 70124 Bari, Italy. Tel.: +39 080 5478326; fax: +39 080 5478310.
E-mail addresses: nico@histology.uniba.it (B. Nico), ribatti@anatomia.uniba.it (D. Ribatti).
0959-8049/$ - see front matter
doi:10.1016/j.ejca.2011.10.022

disease. Moreover, high levels of vascular endothelial growth factor (VEGF) are associated with adverse prognosis.[2]

Little data are available concerning angiogenesis in PCNSL. Takeuchi et al.[3] investigated the expression of VEGF in lymphoma cells and correlated it to microvascular density in 19 patients with PCNSL. They demonstrated that microvascular density was significantly higher in cases immunoreactive to VEGF and that VEGF expression was associated with a longer survival and blood–brain barrier (BBB) alteration. Brain oedema is one of the most serious complications of this tumour and perifocal oedema has been described in both tumoural areas and surrounding brain tissue, where resident microglia and astrocytes are markedly activated.[4]

The aquaporins (AQPs) are a family of water-channel proteins and at least 13 AQPs have been identified and are widely expressed in various fluid-transporting epithelial and endothelial cells in mammals.[5] AQP-1, AQP-4 and AQP-9 have been identified in the brain and AQP-4 is the most important AQP family member involved in brain oedema formation after injury or other brain diseases.[6] In normal brain tissue, AQP4 is mainly expressed in a polarised way by astrocytic endfoot processes enveloping the vessels and it controls the bidirectional water flux at BBB side[7] by exerting a protective role counteracting the vasogenic oedema.[8]

AQP4 expression is correlated to BBB integrity and function,[9] and its expression changes in the neurological disease affecting the BBB.[10,11] In glioblastoma, AQP4 is strongly up-regulated and redistributed across the surfaces of tumour cell and peritumoural oedema is correlated with AQP4 expression.[11,12]

AQPs are involved in tumour growth, angiogenesis and metastatic processes suggesting a potential therapeutic approach in tumour treatment by antagonising their biological activities.[13] No literature data are available concerning the expression of AQP4 in PCNSL and the relationship between AQP4 expression and the morphological characteristics of tumour blood vessels.

In this study, we have evaluated AQP4 expression in bioptic specimens of 24 human diffuse large B-cell PCNSL and we have correlated AQP4 expression to the tumour cells proliferative index, estimated by Ki-67 expression by tumour cells. Moreover, we have studied the morphological features of the tumour microvessels, by means of confocal laser microscopy analysis of double stained microvessels utilising a panel of specific antibodies (anti-factor VIII related antigen and anti-CD31 as endothelial markers; anti-desmin as a pericyte marker; anti-AQP4 and anti-GFAP as glial markers, and anti-CD20 as a tumour cell marker).

2. Materials and methods

2.1. Patients and tissue samples

The clinical and anatomical features of the patients investigated in this study are reported in Table 1. All patients were affected by histologically proven primary human diffuse large B-cell PCNSL. Surgical specimens were fixed in 4% formaldehyde, routinely processed and paraffin-embedded. Three-micrometre thick sections were prepared and routinely stained with Haematoxylin and Eosin; additional sections, collected on superfrost plus slides, were used for immunohistochemical analysis. Peripheral areas, distant 1–3 mm from the edge of the lesion and devoid of tumour cells were used as internal control. Three samples of histologically normal brain removed in the course of surgical exposure were used as control.

2.2. AQP4 and glial fibrillary acidid protein (GFAP) immunocytochemistry

Four micrometre histological sections collected on poly-L-lysine coated slides (Sigma Chemical, St. Louis, MO, USA) were deparaffinised, rehydrated in a xylene-graded alcohol scale and then rinsed for 10 min in 0.1 M phosphate-buffered saline (PBS). The sections were treated after blocking with 1% bovine serum albumin in TBS for 10 min and then sequentially incubated with (i) primary rabbit anti-AQP4 (Santa Cruz Biotechnology, Santa Cruz, CA, USA), and mouse anti-GFAP (Novocastra, Newcastle, UK) antibodies diluted 1:25 and 1:50 in TBS overnight at 4 °C; (ii) secondary antibodies biotin-labelled swine anti-rabbit and swine anti-mouse IgG (Vector Inc., Burlingame, CA), followed by streptavidin-peroxidase conjugate (Vector Inc.). The developing reaction was performed in 0.05 M acetate buffer pH 5.1, 0.02% 3-amino-9-ethylcarbazole grade II (Sigma Chemical Co.) and 0.05% H_2O_2. Sections were then washed in the same buffer, counterstained with Mayer's haematoxylin for 1 min and mounted in buffered glycerine. Negative controls, obtained by substituting normal rabbit serum and normal mouse serum for AQP4 and GFAP primary antibodies, showed no staining of the sections.

Immunohistochemical reactions using a monoclonal antibody anti-Ki-67 (clone Mib1, diluted 1:100, DAKO, Glostrup, Denmark) were performed in an automated immunostainer (Ventana BenchMark Auto-Stainer, Ventana Medical Systems, Tucson, AZ, USA). Ki-67 was scored by evaluating the percentage of stained nuclei, counting positive nuclei in 10 separate fields at 400× magnification in the tumour areas with the highest density of positive nuclei (Table 1).

2.3. Morphometric analysis of AQP4 expression

Morphometric analysis was performed by two independent observers (BN and VL) on nine randomly selected fields every three sections, obtained from the biopsy specimens of each patient, observed at 400× magnification with an Olympus photomicroscope, by using an Image Analysis software (Olympus Italia, Rozzano, Italy). The percent of AQP4 labelled areas were evaluated. Both the extent (relative number of $AQP4^+$ cells) and the intensity of staining were taken into account: – not detected; +, <1% positive cells; ++, 1–10% positive cells with slight to moderate staining; +++, 10–50% positive cells with moderate to marked staining; ++++, >50% positive cells with moderate to marked staining. The mean value in each image from the section, the final mean value for all the images and the standard deviation (SD) were calculated. The statistical significance of the differences between the mean values of the percent labelled areas between patients with a high Ki-67 index as compared with low Ki-67 index and control brain tissues was determined by the Student's *t* test in GraphPad Prism 3.0 software (GraphPad

Table 1 – Clinical and anatomical features of patients and Ki -67 tumour proliferative index.

Case	Sex	Age (years)	Tumour location	Ki-67
1	M	72	Basal ganglia	90
2	F	75	Temporal lobe	70
3	M	82	Occipital lobe	40
4	M	74	Occipital lobe	75
5	M	72	Parieto-temporal lobe	60
6	F	65	Basal ganglia and parietal lobe	40
7	M	65	Assial and extraassial	35
8	M	40	Parieto-frontal lobe	80
9	M	72	Frontal lobe and corpus callosum	75
10	F	70	D9–D10	40
11	M	69	Parietal lobe	95
12	M	64	Parieto-frontal lobe	80
13	M	73	Parieto-frontal lobe	80
14	F	65	Cerebellar	80
15	M	58	Occipital lobe	80
16	M	72	Parietal lobe	45
17	F	64	Parieto-occipital lobe	80
18	M	37	Basal ganglia	80
19	F	38	Multiple intra-cerebral	65
20	M	44	Cerebellar	40
21	F	61	Parieto-frontal lobe	25
22	F	67	Basal ganglia	80
23	M	58	Temporal lobe	70
24	M	66	Frontal lobe	85

software, La Jolla, CA, USA). The findings were considered significant at P values <0.05.

2.4. *Dual immunofluorescence-confocal laser scanning microscopy*

Twelve micrometre thick deparaffinised brain sections were incubated for 30 min in a blocking buffer [BB; phosphate-buffered saline (PBS), pH 7.4, 1% bovine serum albumin, 2% foetal calf serum] and exposed to primary antibodies: (i) rabbit anti-AQP4 (Santa Cruz Biotechnology), and mouse anti-CD20 (Dako Corporation, Glöstrup, Denmark), diluted respectively 1:50 and 1:200 in BB, overnight at 4 °C; (ii) rabbit anti-AQP4 and rat anti-CD31 (AbD Serotec, Oxford, UK), diluted 1:50 and 1:5 in BB, overnight at 4 °C; (iii) rabbit anti-FVIII (Dako Corporation, Milan, Italy), and mouse anti-CD20, diluted 1:100 and 1:200 in BB, overnight at 4 °C; (iv) rabbit anti-FVIII and mouse anti-GFAP (Novocastra, Newcastle, UK), diluted respectively 1:100 and 1:50 in BB, overnight at 4 °C; (v) rabbit anti-FVIII and mouse anti-desmin, (Dako Corporation) diluted respectively 1:100 and 1:10 in BB, overnight at 4 °C. After washing in PBS the sections were incubated for 2 h with the secondary antibodies: (i) Alexa Fluor 555 goat anti-rabbit antibody (Invitrogen, Carlsbad, CA, USA) and Alexa Fluor 488 goat anti-mouse antibody (Invitrogen, Carlsbad), diluted 1:300 in BB for AQP4 and CD20 dual localisation; (ii) Alexa Fluor 555 goat anti-rabbit antibody and Alexa Fluor 488 goat anti-rat antibodies (Invitrogen, Carlsbad) diluted 1:300 in BB for AQP4 and CD31 dual localisation; (iii) Alexa Fluor 555 goat anti-rabbit and Alexa Fluor 488 goat anti-mouse antibodies (Invitrogen, Carlsbad), diluted 1:300 in BB for FVIII and CD20 dual localisation; (iv) Alexa Fluor 555 goat anti-rabbit and Alexa Fluor 488 goat anti-mouse antibodies (Invitrogen, Carlsbad), diluted 1:300 in BB for FVIII and GFAP dual localisation; (v) Alexa Fluor 555 goat anti-rabbit and Alexa Fluor 488 goat anti-mouse antibodies (Invitrogen, Carlsbad), diluted 1:300 in BB for FVIII and desmin dual localisation. All the samples were incubated for 5 min with 0.01% TO-PRO-3 (Invitrogen, Carlsbad) for nuclear staining and mounted in Vectashield (Vector Inc., Burlingame, CA, USA). Negative controls, obtained by substituting primary antibodies with normal rabbit serum for AQP4 and FVIII; normal mouse serum for CD20, desmin and GFAP; normal rat serum for CD31, showed no staining of the sections. The sections were examined under a Leica TCS SP2 (Leica, Wetzlar, Germany) confocal laser scanning microscope using 40× and 63× objective lenses with either 1× or 2× zoom factors. A sequential scan procedure was applied during image acquisition of the two fluorophores. Confocal images were taken at 200 nm intervals through the z-axis of the section covering a total depth of 10 μm. Images from individual optical planes and multiple serial optical sections were analysed, digitally recorded and stored as TIFF files using Adobe Photoshop software (Adobe Systems Inc., San Jose, CA, USA).

3. Results

3.1. *AQP4 immunocytochemical expression correlates with proliferation within PCNSL*

AQP4 showed marked differences in its expression. In the peripheral areas, distant 1–3 mm from the edge of the lesion and devoid of tumour cells, used as internal control (Fig. 1A), and in normal brain (Fig. 1B) AQP4 showed a perivascular uniform staining labelling the glial processes and forming a continuous perivascular sheath. In the tumour areas

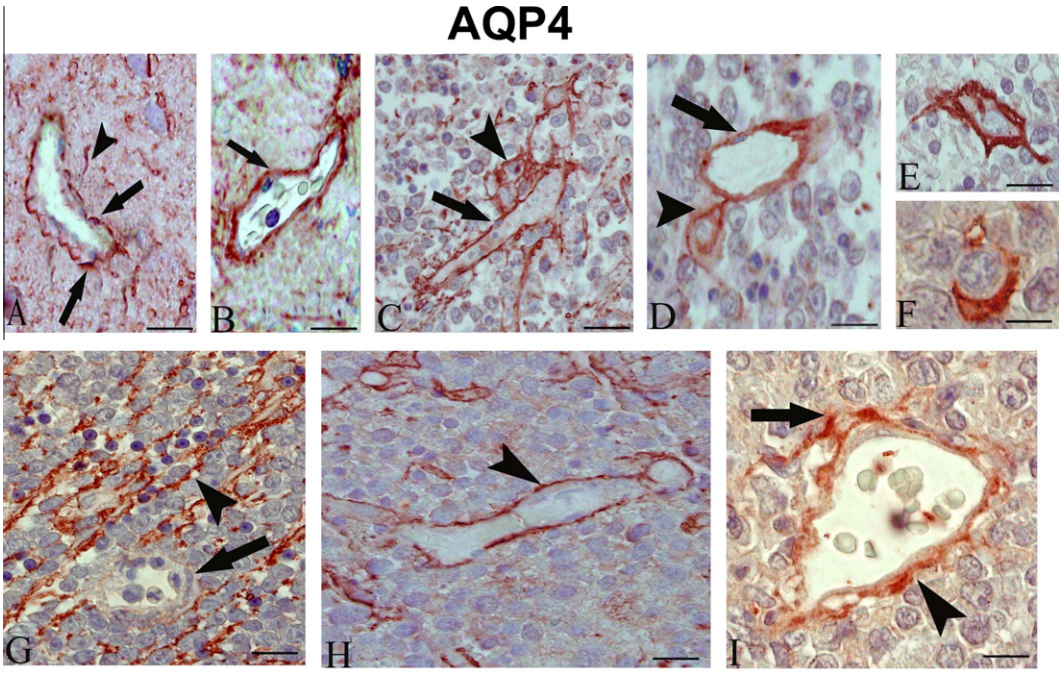

Fig. 1 – Aquaporin-4 (AQP4) immunocytochemical expression in internal healthy (A) and in control (B) brain tissues and in primary central nervous system lymphoma (PCNSL) with high (C–G) and low (H–I) Ki-67 index. (A and B) Control brain sections showing a continuous perivascular AQP4 staining of glial endfeet surrounding (arrow) and touching (A, arrowhead) the vessel wall. (C–G) Tumour brain sections with high Ki-67 index showing AQP4-labelled endothelial cells (C and D arrow), and clusters of labelled tumour cells close to the vessels (C and D arrowhead), and expressing a cytoplasmic AQP4 staining (E and F). AQP4 staining (G, arrowhead) is detectable between rows of tumour cells including an unlabelled vessel (G, arrow). (H and I) Tumour brain sections with low Ki-67 index showing a restored AQP4 perivascular labelling (H and I, arrowhead). A labelled AQP4 tumour cell (I, arrow) close to a vessel wall is recognisable. Scale bar: A, B, C, G, and H, 25 μm; D and I, 16 μm; E and F, 10 μm.

from patients with a high Ki-67 index (between 70% and 90%), a stronger AQP4 expression was recognisable in endothelial cells without differences correlated to the vascular calibre (Fig. 1C and D) and tumour cells in both cytoplasm (Fig. 1E and F) and plasma membrane (Fig. 1F). Clusters of tumour cells intensely reactive to AQP4 were observed close to the vessel wall or connected by their cytoplasmic expansions to AQP4$^+$ endothelial cells (Fig. 1C and D). Tumour vessels negative to AQP4 on vascular and perivascular sides were also recognisable (Fig. 1G, arrow). Moreover, immunoreactivity to AQP4 was detected in the neuropile between the tumour cells, forming long rows separated by AQP4$^+$ cell processes (Fig. 1G). In the tumour areas from patients with a low Ki-67 index (between 25% and 40%), AQP4 labelling was appreciable on the vascular abluminal side (Fig. 1H and I) and few AQP4$^+$ tumour cells were recognisable close to the vessel wall (Fig. 1H and I). Morphometric analysis showed a significant increase of AQP4 expression in the tumour areas from patients with a high Ki-67 index as compared with low Ki-67 index and internal healthy as well as control brain tissues (Fig. 2). Tumour cells immunoreactive to AQP4 appeared elongated with thin cytoplasmic protrusions (Fig. 3A) or round-shaped (Fig. 3E). In both tumour cell types, after dual immunofluorescence a merge orange signal for CD20 and AQP4 proteins was recognisable on the plasma membrane of a single cell (Fig. 3B–D, F–H, arrows).

3.2. *Morphological heterogeneity of tumour blood vessels*

While in healthy brain tissue, vessels were lined by CD31$^+$ endothelial cells surrounded by AQP4$^+$ glial perivascular endfeet (Fig. 4G), tumour vessels were heterogenous, since they were lined by CD20$^+$ tumour cells and FVIII$^+$ endothelial cells (Fig. 4A and B) or by CD20$^+$ and FVIII$^+$ (Fig. 4A), AQP4$^+$ and CD31$^+$ (Fig. 4C–F) or AQP4$^+$ and CD20$^+$ (Fig. 4F–H, arrowhead) tumour cells. Finally, tumour vessels lined by GFAP$^+$ endothelial cells surrounded by GFAP$^+$ tumour cells were appreciable (Fig. 5A). After dual immunofluorescence, vessels of tumours with a high Ki-67 index, appeared to be lined by a single endothelial cell with a merge orange signal, expression of FVIII and GFAP co-localisation, surrounded by irregularly shaped tumour cells immunoreactive to GFAP (Fig. 5B and C). Moreover, tumour vessels lined by FVIII$^+$ endothelial cells appeared surrounded by rows of tumour cells arranged in a circle with a separate GFAP and FVIII immunoreactivity (Fig. 5D), or by GFAP$^+$ tumour cells (Fig. 5E). Tumours with a low Ki-67 index showed vessels with FVIII$^+$ endothelial cells surrounded by a continuous layer of GFAP$^+$ glial processes (Fig. 5F). In the peripheral areas, distant 1–3 mm from the edge of the lesion used as internal control (Fig. 1A), and in normal brain (Fig. 1B) vessels were lined by FVIII$^+$ endothelial cells and GFAP$^+$ glial processes enveloping the vessels and scattered in the neuropile.

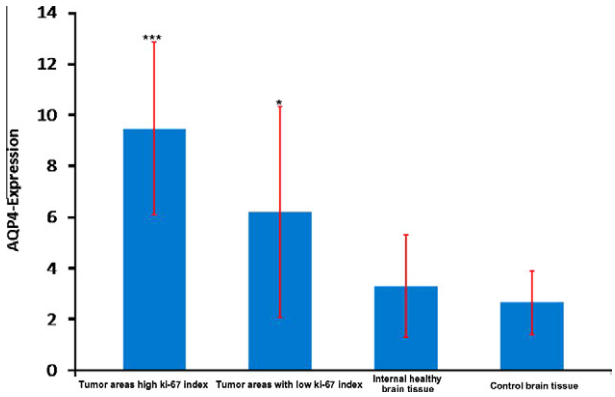

Fig. 2 – Morphometric analysis of AQP4 expression shows significant differences in the AQP4 expression between the tumour areas from patients with a high Ki-67 index as compared with low Ki-67 index and internal healthy and control brain tissues. $^{***}P < 0.001$, $^{*}P < 0.05$ versus control brain tissues.

In the central tumour areas of both tumours with high and low Ki-67-index, vessels were immunoreactive only to FVIII, but not to the pericyte marker desmin (Fig. 6A), while in the peripheral tumour areas vessels they were immunoreactive to desmin in short tracts of their wall (Fig. 6B and C). Otherwise, in the peripheral areas, distant 1–3 mm from the edge of the lesion used as internal control (Fig. 6D), and in normal brain (Fig. 6E), vessels showed a luminal immunoreactivity to FVIII and an abluminal immunoreactivity to desmin with a pointed pattern of expression along the entire vessel wall.

4. Discussion

4.1. *AQP4 expression in PCNSL*

In this study, we have demonstrated for the first time that in bioptic specimens from patients affected by primary human diffuse large-B cell PCNSL, a high AQP4 expression was correlated with a high Ki-67 index, as compared with healthy brain tissue, while in the tumour areas from patients with a low Ki-67 index, AQP4 expression was low. Moreover, AQP4 marked tumour and endothelial cells in cytoplasm

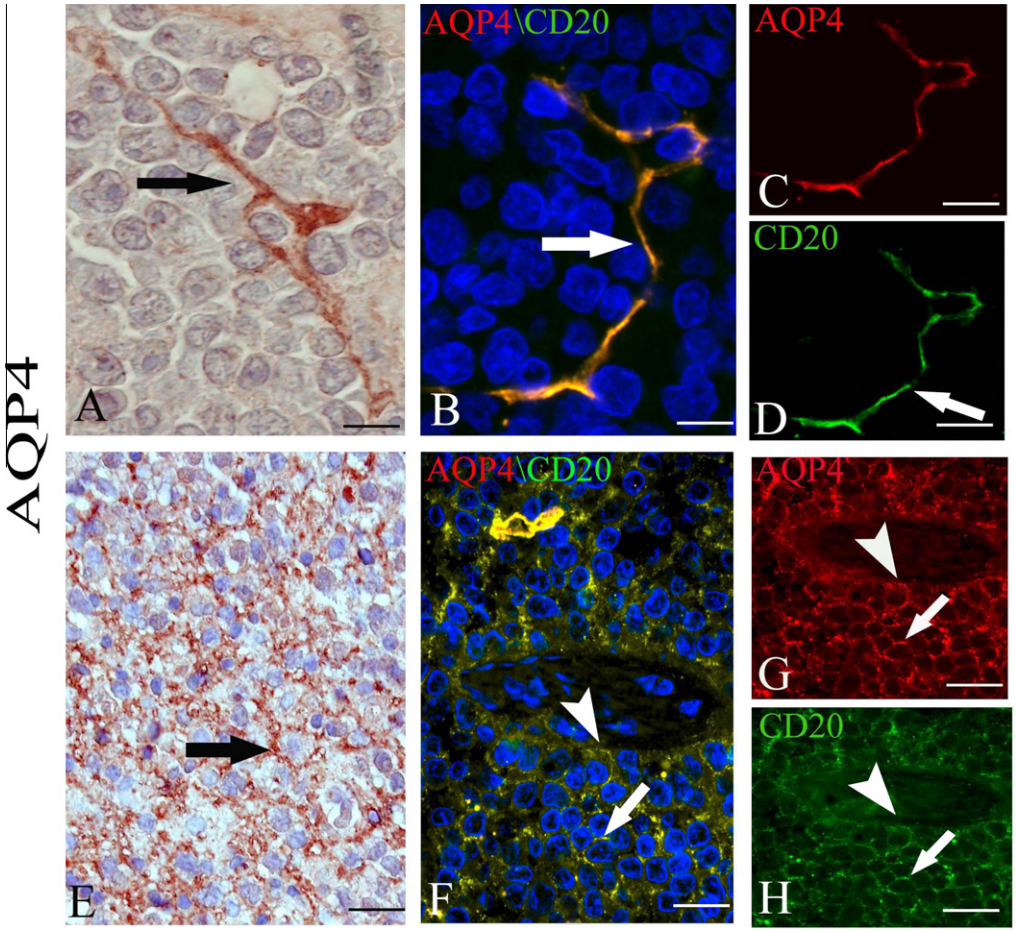

Fig. 3 – AQP4 immunohistochemistry (A and E) and AQP4 (in red)/CD20 (in green) (B–D and F–H) confocal dual immunofluorescence. Elongated (A) or rounded (E) tumour cells expressing AQP4 staining in their cytoplasm (A, arrow) and plasma membrane (E, arrow), are labelled by both anti-CD20 (D and H, arrow) and anti-AQP4 antibodies, with a merge fluorescence signal of colocalisation on a single cell (B and F, arrow). A vessel lined by tumour cells with a fluorescent signal expression of CD20 (H, arrowhead) and AQP4 (G, arrowhead) colocalisation is shown in F (arrowhead). Scale bar: A–D, 16 μm; E–H, 25 μm. (For interpretation of the references to colour in this figure legend, the reader is referred to the web version of this article.)

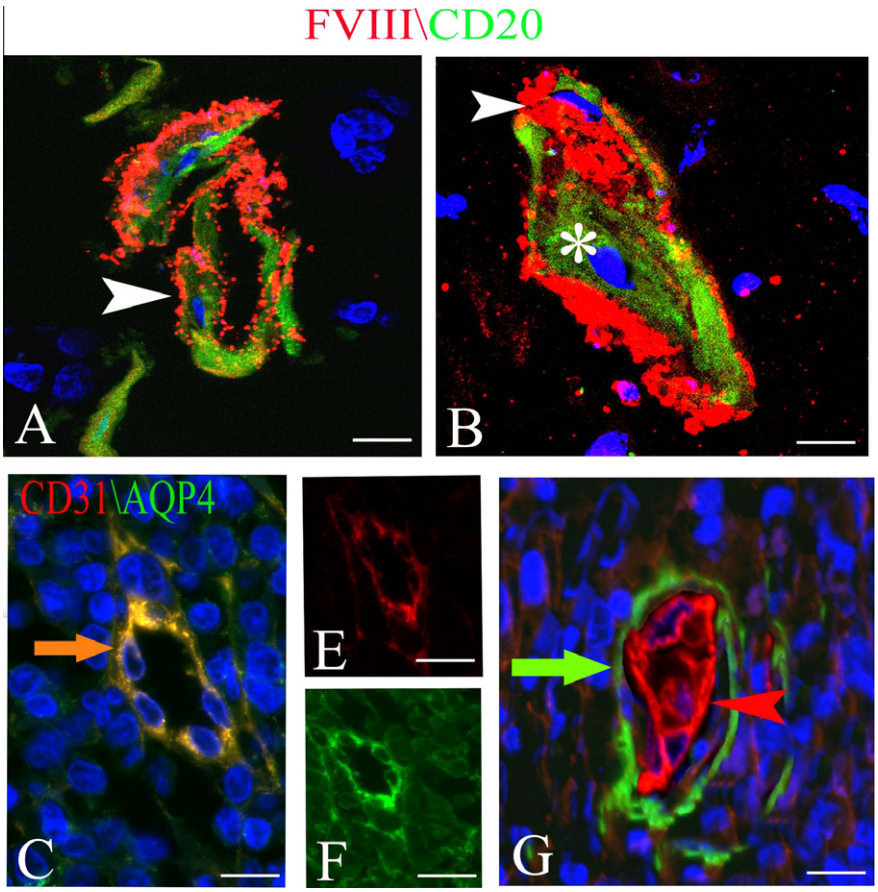

Fig. 4 – (A and B) Confocal dual immunofluorescence reaction of FVIII (in red)/CD20 (in green) in tumour sections. The vessels are lined by FVIII fluorescence endothelial cells (A, arrowhead) and CD20 labelled tumour cells (B, asterisk). (C–G) Confocal dual immunofluorescence reaction of CD31 (in red)/AQP4 (in green) in tumour (C and F) and control (G) sections. A merge orange signal of AQP4/CD31 colocalisation is detectable in the tumour vessel on a single endothelial cell (C, arrow). A separate endothelial CD31 (G, arrowhead) and glial AQP4 (G, arrow) fluorescence signal is detectable in control tissue (G). Scale bar: A–G, 16 μm. (For interpretation of the references to colour in this figure legend, the reader is referred to the web version of this article.)

and plasma membrane in patients with a high Ki-67 index, while in patients with low Ki-67 index few tumour cells were positive to AQP-4, and endothelial cells showed AQP-4 expression on their abluminal side. Heterogeneous tumour location did not influence both Ki-67 index and AQP4 expression.

AQP4 is a component of the dystrophin complex which is expressed predominantly in the astrocytic foot processes near blood vessels, where it controls brain water exchanges acting as a main component of the BBB.[7,14] The perivascular glial polarised AQP4 expression is maintained by the links between the dystrophin complex and extracellular matrix,[15,16] and changes in the AQP4 polarisation are important in the pathogenesis of cerebral oedema.[6]

It has been demonstrated that AQP4 is strongly expressed in GBM in combination with loss of its polarised expression around the vessels and redistribution on the glioma cell membranes.[11,17] Moreover, AQP4 over-expression correlates with vasogenic oedema.[8,11]

Previously, we have demonstrated in GBM bioptic specimens that in the relapse after chemotherapy and radiotherapy, AQP4 expression is reduced in parallel with VEGF–VEGF-receptor-2 (VEGFR-2) expression as compared with primary tumours, and in peripheral areas of relapsed tumour AQP4 mimick normal findings of perivascular rearrangements.[18] These data indicate that in GBM chemotherapy and radiotherapy induce a down-regulation in AQP4 expression restoring its perivascular rearrangement and suggest its potential role in the resolution of brain oedema. Moreover, the normally polarised rearrangement of AQP4 in peripheral areas in tumour specimens obtained after combined chemotherapy and radiotherapy could be due to normalisation of tumour blood vessels.

AQP4 is involved in the cytoskeleton organisation through a link with α-syntrophyn[17] and in the astrocytes of AQP4-knockdown mouse a remarkable actin cytoskeleton rearrangement and impaired cell migration has been reported.[21,22] In GBM, AQP4 redistribution has been correlated with tumour cell migratory capability[19,20] and AQP4 colocalised with protein kinase C to the leading edge of invading glioma cells,[23] suggesting that AQP4, besides water transport, might be involved in tumour malignancy and progression.

In primary human diffuse large-B cell PCNSL, high AQ4 expression might favour tumour progression in term of both tumour cell proliferation and migration. In fact, reduced intercellular adhesion, followed by cell invasion, are essential

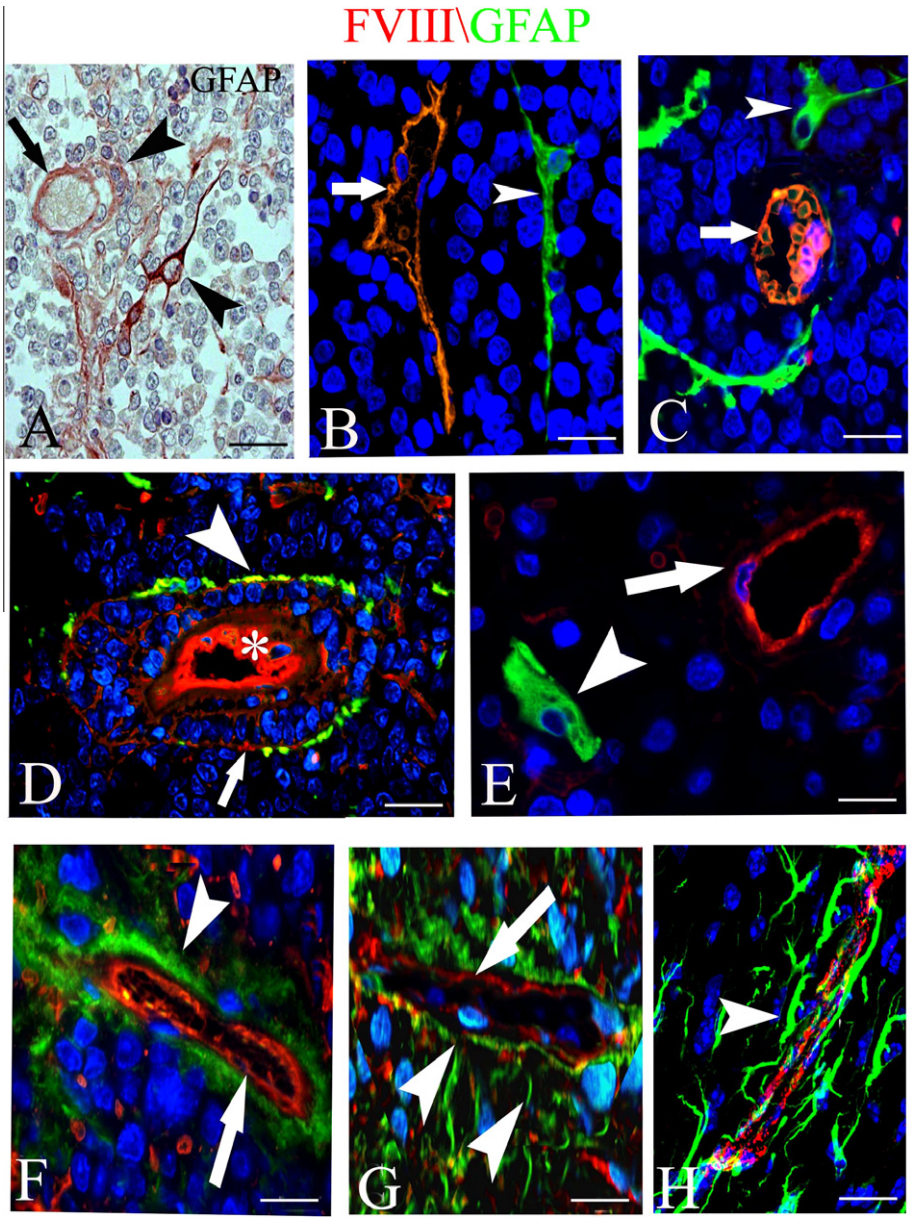

Fig. 5 – Glial fibrillary acidid protein (GFAP) immunohistochemistry (A) and FVIII (in red)/GFAP (in green) (B–G) confocal dual immunofluorescence. (A) Tumour vessels are lined by GFAP marked endothelial cells (arrow) surrounded by GFAP stained tumour cells (arrowhead). (B–E) Tumour vessels with high Ki-67 index show an orange fluorescence signal expression of FVIII/GFAP colocalisation on a single endothelial cell (B and C, arrow) near to GFAP labelled tumour cells (B and C arrowhead). Tumour vessels with thickened (D, asterisk) or thin (E, arrow) endothelium positive to FVIII, surrounded by tumour cells expressing a separate GFAP (D and E, arrowhead) and FVIII fluorescence (D, arrow), are recognisable. (F–H) Tumour vessels with low Ki-67 index (F), internal healthy (G), and control brain (H) tissues showing an endothelial FVIII red fluorescence (arrow) are enveloped by a continuous layer of GFAP green fluorescence glial processes (arrowhead). Scale bar: A, 25 μm; B–H, 16 μm. (For interpretation of the references to colour in this figure legend, the reader is referred to the web version of this article.)

steps in the progression from local malignancy to metastatic disease. Moreover, AQP4 by induction of cerebral oedema by AQP4 is another negative prognostic factor.

4.2. *Vascular heterogeneity in PCNSL*

Structural microvessel abnormalities have been described in some lymphoma subtypes. Hyek et al.[24] demonstrated that aggressive lymphomas express an increased number of blood vessels, but also a relatively increased number of immature vessels lacking pericytes, in comparison with reactive lymph nodes and indolent lymphomas.

Here, we have demonstrated that tumour vessels showed a high grade of heterogeneity. Different types of vessels were recognisable formed by: $CD20^+$ tumour cells and $FVIII^+$ endothelial cells; $AQP4^+$ tumour cells and $CD31^+$ endothelial cells;

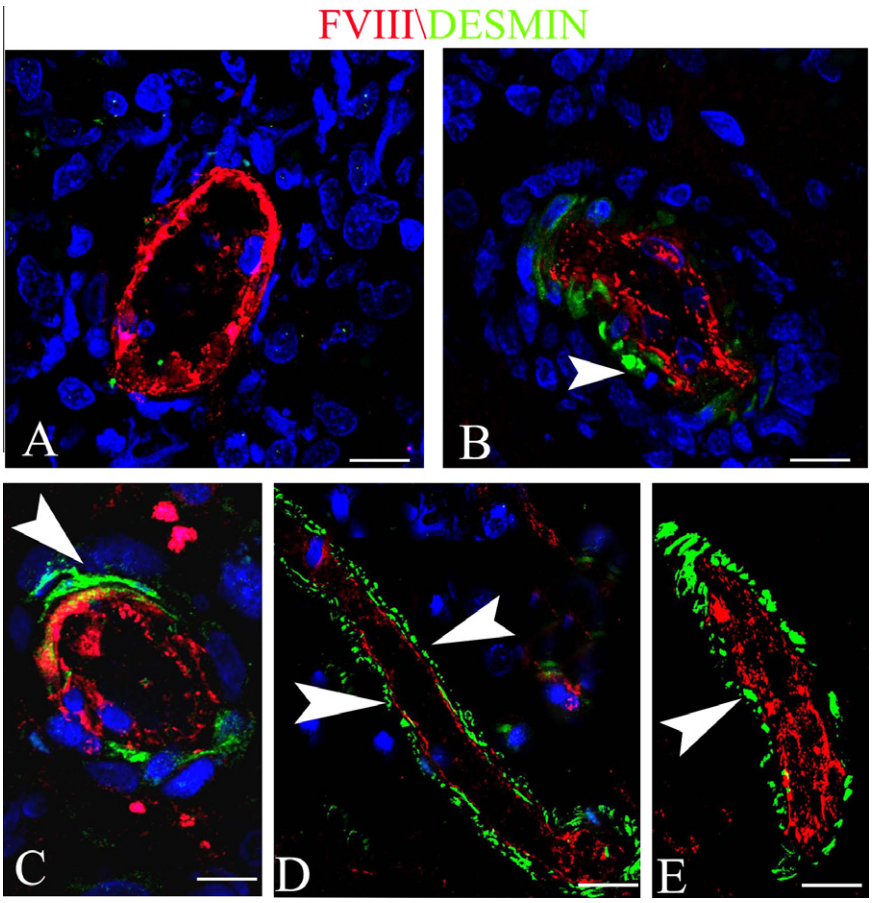

Fig. 6 – Confocal dual immunofluorescence reaction of FVIII (in red)/desmin (in green) in tumour (A–C) and internal healthy (D) and control (E) brain sections. Vessels from inner tumoural areas (A) show only a FVIII signal, while tumour vessels from peripheral tumoural areas (B and C) show a FVIII signal and in short tracts are subtended by a desmin fluorescence (arrowhead). (D and E) Control brain sections show vessels lined by a FVIII endothelium enveloped by a continuous desmin reactivity with a pointed pattern expression along the abluminal side (arrowhead). Scale bar: A–E, 16 μm.

tumour cells positive to both CD20 and AQP4; GFAP$^+$ endothelial cells surrounded by GFAP$^+$ tumour cells.

Literature data have reported that a common feature of several types of tumours is the heterogeneity of their microvascular in terms of different types of cells involved in the formation of the vessel wall. Tumour cells from aggressive cancers can mimic the activities of endothelial cells by forming vascular-like networks.[25–27] The formation of vascular channels by tumour cells as a result of 'vasculogenic mimicry', i.e. the *de novo* generation of blood vessels without the participation of endothelial cells, has been described for melanomas, sarcomas, breast, ovary, lung and prostate carcinomas.[28,29]

It has been also suggested that tumour cells and endothelial cells may derive from a multipotent haemangioblastic precursor cell. Gunsilius et al.[27] have shown that BCR-ABL translocation can be detected in a subgroup of endothelial cells generated *in vitro* from bone marrow and peripheral blood specimens obtained from patients with myeloid leukaemia, suggesting the existence of a common malignant precursor cell.

Circulating endothelial cells and VEGF levels correlate with tumour volume in SCID mice bearing human lymphoma.[30] Igreja et al.[31] found increased circulating endothelial precursor cells in patients with aggressive non-Hodgkin's lymphomas and demonstrated that the levels of circulating endothelial progenitor cells decreased following complete response to treatment. Moreover, the presence of circulating endothelial progenitor cells in lymphomas provides a useful angiogenesis-specific biomarker to evaluate the treatment response following antiangiogenic therapy.

An alternative hypothesis concerns the possibility of the formation of hybrid vessels by the fusion of malignant cells and endothelial cells.[32–34] Holash et al.[35] reported that tumour cells migrate to host organ blood vessels in sites of metastases, or in vascularised organs such as the brain, and initiate blood vessel growth as opposed to classic angiogenesis.

The ability of cancer stem-like cells to directly contribute to the tumour vasculature by endothelial cell differentiation has been described in ovarian cancer[36] in B-cell lymphomas,[26] in human neuroblastoma[37] and in human GBM.[33,38]

Streubel et al.[26] demonstrated that 15–85% of microvascular endothelial cells in B-cell lymphomas harboured lymphoma-specific genetic alterations consisting not only of B-cell-specific translocation of IGH, but also secondary genetic alterations in follicular lymphomas. These cytogenetic abnormalities in lymphoma endothelial cells suggested that

lymphoma microvessels are active players in tumour progression and dissemination and that microvascular endothelial cells in B-cell lymphomas are in part tumour-related, raising the possibility that a portion of the lymphoma endothelial cells may be derived from a common progenitor in the bone marrow. Huang et al.[39] have identified the expression of a transcript called T cell Ig and mucin domain-containing molecule 3 (Tim-3) in microvessels of diffuse large B cell lymphomas and peripheral T cell lymphomas, but not in reactive lymph nodes, suggesting that the lymphoma endothelium may act as a functional barrier facilitating the establishment of lymphoma immune tolerance.

Pezzolo et al.[37] demonstrated that a subset of human MYCN-amplified neuroblastoma tumours contains microvessels formed by the malignant cells themselves, as demonstrated by the detection of MYCN amplification in $CD31^+$ or $CD105^+$ endothelial cells. Moreover, in xenografts of the HTLA-230 human neuroblastoma cell line, they demonstrated that approximately 70% of vessels stained for human CD31, but not murine CD34, and displayed MYCN amplification, thus proving their tumour origin.

Ricci-Vitiani et al.[38] demonstrated that 60.7% of endothelial cells in glioblastoma carry the same genetic alteration of tumour cells, indicating that tumour vascular endothelium has a neoplastic origin. A subset of glioblastoma stem-like cells (GSC) *in vitro* generated a progeny with phenotypic and functional features of endothelial cells and orthotopic or subcutaneous injection of GSCs in immunocompromised mice produced tumour xenografts with vessels composed of human endothelial cells.[38] Moreover, selective targeting of endothelial cells generated by GSC in mouse xenografts resulted in tumour reduction and degeneration. In parallel, Wang et al.[33] have shown that a subpopulation of cells within glioblastoma can give rise to endothelial cells and that the $CD133^+$ cancer stem cell-like fraction is multipotent and capable of differentiation along tumour and endothelial lineages, via an intermediate $CD133^+/CD144^+$ progenitor cell. Moreover, they demonstrated that exposure to the anti-VEGF monoclonal antibody bevacizumab inhibited the maturation of tumour endothelial progenitors into endothelial cells, but not the differentiation of $CD133^+$ cells into endothelial progenitors. A last possibility is related to a gene transfer by means of the uptake of apoptotic bodies from tumour cells by neighbouring cells.[40,41]

Our data suggest that 'vasculogenic mimicry' might occur in PCNSL, representing an incomplete differentiation of cancer stem-like cells towards the endothelial lineage, as indicated by the aberrant mixed phenotype of tumour cells generated by the subset of $CD20^+/FVIII^+$ and $CD20^+/AQP4^+$ tumour cells.

The absence of periendothelial coverage by pericytes in the central tumour areas as compared to peripheral ones, is an expression of the immaturity of blood vessels in the tumour core. In fact, in this area the high proliferative index of tumour cells is also responsible for a high proliferation of blood vessels associated to their incomplete structure also in term of pericyte coverage. Pericyte deficiency could be partly responsible for vessel abnormalities in tumour blood vessels[42] and partial dissociation of pericytes[43] contribute to increased tumour vascular permeability and oedema.

Overall, the data presented in this study have confirmed the importance of AQP4 as a marker of tumour progression in primary human diffuse large-B cell PCNSL due to its involvement in cerebral oedema formation and resolution and tumour cell migratory activity. Moreover, the importance and clinical relevance of neoangiogenesis in the pathogenesis of lymphoproliferative diseases has been confirmed, as documented by the extreme heterogeneity and complexity of vasculature, due to different cells with mixed phenotypic characteristics involved in the formation of tumour blood vessels. Further knowledge about the morpho-functional properties of tumour blood vessels is essential for the development of more appropriate antivascular therapies able to target these hybrid and atypic blood vessels.

Author contribution statement

B.N., T.A., R.T., V.L., S.R. and R.S. carried out the experiments. B.N., P.T., G.S., A.V. and D.R. analysed and interpreted data. B.N. and D.R. were responsible for the study design and wrote the paper. All authors were involved in editing the paper and had final approval of the submitted version.

Conflict of interest statement

None declared.

Acknowledgments

This work was supported by the Associazione Italiana per la Ricerca sul cancro (AIRC), Investigator Grant and Special Program Molecular Clinical Oncology 5 per mille n. 9965, Milan, Italy.

REFERENCES

1. Paulus W. Classification, pathogenesis and molecular pathology of primary CNS lymphomas. *J Neurooncol* 1999;**43**:203–8.
2. Koster A, Raemaekers J. Angiogenesis in malignant lymphoma. *Curr Opin Oncol* 2005;**17**:611–6.
3. Takeuchi H, Matsuda K, Kitai R, Sato K, Kubota T. Angiogenesis in primary central nervous system lymphoma (PCNSL). *J Neurooncol* 2007;**84**:141–5.
4. Schlegel U, Schmidt-Wolf IG, Deckert M. Primary CNS lymphoma: clinical presentation, pathological classification, molecular pathogenesis and treatment. Review. *J Neurol Sci* 2000;**181**:1–12.
5. Agree P. Nobel lecture. Aquaporin water channel. *Biosci Rep* 2004;**24**:127–63.
6. Badaut J, Lasbennes F, Magistretti PJ, Regli L. Aquaporins in brain: distribution, physiology, and pathophysiology. *J Cerebr Blood Flow Metab* 2002;**22**:367–78.
7. Nico B, Frigeri A, Nicchia GP, et al. Role of aquaporin-4 water channel in the development and integrity of the blood–brain barrier. *J Cell Sci* 2001;**114**:1297–307.
8. Saadoun S, Papadopoulos MC, Davies DC, Krishna S, Bell BA. Aquaporin-4 expression is increased in oedematous human brain tumors. *J Neurol Neurosurg Psychiatry* 2002;**72**:262–5.

9. Nico B, Frigeri A, Nicchia GP, et al. Severe alterations of endothelial and glial cells in the blood–brain barrier of dystrophic mice. *Glia* 2003;**42**:235–51.
10. Medici V, Frassoni C, Tassi L, Sprefico R, Garbelli R. Aquaporin 4 expression in control and epileptic human cerebral cortex. *Brain Res* 2001;**1367**:330–9.
11. Warth A, Simon P, Capper D, et al. Expression pattern of the water channel aquaporin-4 in human gliomas is associated with blood–brain barrier disturbance but not with patient survival. *J Neurosci Res* 2007;**85**:1336–45.
12. Mou K, Chen M, Mao Q, et al. AQP-4 in peritumoral edematous tissue is correlated with the degree of glioma and with expression of VEGF and HIF-alpha. *J Neuroncol* 2010;**100**:375–83.
13. Nico B, Ribatti D. Aquaporins in tumor growth and angiogenesis. *Cancer Lett* 2010;**294**:135–8.
14. Nielsen S, Nagelhus EA, Amiry-Moghaddam M, et al. Specialized membrane domains for water transport in glial cells: high-resolution immunogold cytochemistry of aquaporin-4 in rat brain. *J Neurosci* 1997;**17**:171–80.
15. Nicchia GP, Rossi A, Nudel U, Svelto M, Frigeri A. Dystrophin-dependent and -independent AQP4 pools are expressed in the mouse brain. *Glia* 2008;**56**:869–76.
16. Nico B, Tamma R, Annese T, et al. Glial dystrophin-associated proteins, laminin and agrin, are downregulated in the brain of mdx mouse. *Lab Invest* 2010;**90**:1645–60.
17. Warth A, Kroger S, Wolburg H. Redistribution of aquaporin 4 in human glioblastoma correlates with loss of agrin immunoreactivity from brain capillary basal laminae. *Acta Neuropathol* 2004;**107**:311–8.
18. Nico B, Mangieri D, Tamma R, et al. Aquaporin-4 contributes to the resolution of peritumoral brain oedema in human glioblastoma multiforme after combined chemotherapy and radiotherapy. *Eur J Cancer* 2009;**45**:3315–25.
19. McCoy E, Sontheimer H. Expression and function of water channels (aquaporins) in migrating malignant astrocytes. *Glia* 2007;**55**:1034–43.
20. Ding T, Gu F, Fu L, Ma YJ. Aquaporin-4 in glioma invasion and an analysis of molecular mechanism. *J Clin Neurosci* 2010;**17**:1359–61.
21. Nicchia GP, Srinivas M, Li W, et al. New possible roles for aquaporin-4 in astrocytes: cell cytoskeleton and functional relationship with connexin 43. *FASEB J* 2005;**19**:1674–6.
22. Saadoun S, Papadopoulos MC, Hara-Chikuma M, Verkman AS. Impairment of angiogenesis and cell migration by targeted aquaporin-1 gene disruption. *Nature* 2005;**434**:786–92.
23. McCoy ES, Haas BR, Sontheneimer H. Water permeability through aquaporin-4 is regulated by protein kinase C and becomes rate-limiting for glioma invasion. *Neuroscience* 2010;**168**:971–81.
24. Hyek E, Chadburn A, Dias S. High grade non-Hodgkin's lymphomas and Hodgkin's disease are associated with increased density of KDR+ SMA (–) immature microvessels. *Blood* 1999;**94**:597a.
25. Maniotis AJ, Folberg R, Hess A, et al. Vascular channel formation by human melanoma cells in vivo and in vitro: vasculogenic mimicry. *Am J Pathol* 1999;**155**:739–52.
26. Streubel B, Chott A, Huber D, et al. Lymphoma-specific genetic aberrations in microvascular endothelial cells in B-cell lymphomas. *N Engl J Med* 2004;**351**:250–9.
27. Gunsilius E, Duba HC, Petzer AL, et al. Evidence from a leukaemia model for maintenance of vascular endothelium by bone marrow-derived endothelial cells. *Lancet* 2000;**355**:1688–91.
28. Hendrix MJ, Seftor EA, Hess AR, Seftor RE. Vasculogenic mimicry and tumour cell plasticity: lessons from melanoma. *Nat Rev Cancer* 2003;**3**:411–21.
29. Dorne B, Hendrix MJ, Paku S, Tovari J, Timar J. Alternative vascularization mechanisms in cancer: pathology and therapeutic implications. *Am J Pathol* 2007;**170**:1–15.
30. Monestiroli S, Mancuso P, Burlini K. Kinetics and viability of circulating endothelial cells as surrogate angiogenesis marker in an animal model of human lymphoma. *Cancer Res* 2001;**61**:4341–4.
31. Igreja C, Courinha M, Cachao AS, et al. Characterization and clinical relevance of circulating and biopsy-derived endothelial progenitor cells in lymphoma patients. *Haematologica* 2007;**92**:469–77.
32. Ying QL, Nichols J, Evans EP, Smith AG. Changing potency by spontaneous fusion. *Nature* 2002;**416**:545–8.
33. Wang R, Chadalavada K, Wilshire J, et al. Glioblastoma stem-like cells give rise to tumour endothelium. *Nature* 2010;**468**:829–33.
34. Vassilopoulos G, Wang PR, Russell DW. Transplanted bone marrow regenerates liver by cell fusion. *Nature* 2003;**422**:901–4.
35. Holash J, Maisonpierre PC, Compton D, et al. Vessel cooption, regression and growth in tumors mediated by angiopoietins and VEGF. *Science* 1999;**284**:1994–8.
36. Alvero AB, Chen R, Fu HH, et al. Molecular phenotyping of human ovarian cancer stem cells unravels the mechanism for repair and chemoresistance. *Cell Cycle* 2009;**8**:158–66.
37. Pezzolo A, Parodi F, Corrias MV, et al. Tumor origin of endothelial cells in human neuroblastoma. *J Clin Oncol* 2007;**25**:376–83.
38. Ricci-Vitiani L, Pallini R, Biffoni M, et al. Tumour vascularization via endothelial differentiation of glioblastoma stem-like cells. *Nature* 2010;**468**:824–8.
39. Huang X, Bai X, Cao Y, et al. Lymphoma endothelium preferentially expresses Tim-3 and facilitates the progression of lymphoma by mediating immune evasion. *J Exp Med* 2010;**207**:505–20.
40. Holmgren L, Szeles A, Rajnavolgy E, et al. Horizontal transfer of DNA by the uptake of apoptotic bodies. *Blood* 1999;**93**:3956–63.
41. Bergsmedh A, Szeles A, Henriksson M, et al. Horizontal transfer of oncogenes by uptake of apoptotic bodies. *Proc Natl Acad Sci USA* 2001;**98**:6407–11.
42. Gerhardt H, Semb H. Pericytes: gatekeepers in tumor cell metastasis? *J Mol Med* 2008;**86**:135–44.
43. Hashizume H, Baluk P, Morikawa S, et al. Openings between defective endothelial cells explain tumor vessel leakiness. *Am J Pathol* 2000;**156**:1363–80.